

Fluctuations in the scrape-off layer and edge plasma of the COMPASS tokamak

J. Seidl¹, K. Jirakova^{1,2}, J. Adamek¹, O. Grover^{1,2}, J. Horacek¹, M. Hron¹, P. Vondracek^{1,3}

¹ Institute of Plasma Physics of the CAS, Prague, Czech Republic

² Faculty of Nuclear Sciences and Physical Engineering, CTU, Prague, Czech Republic

³ Faculty of Mathematics and Physics, Charles University, Prague, Czech Republic

Edge plasma losses in L-mode are dominated by turbulent transport. The transport is non-local and turbulent structures (blobs) carrying hot and dense plasma outwards were detected in the scrape-off layer (SOL) of many tokamaks [1]. Due to their typical shape and Poisson distribution of waiting times, local probability density function (PDF) of density fluctuations forms a positively skewed Gamma distribution [2]. The place where the skewness drops to zero, which is typically found inside the last closed flux surface (LCFS), is often identified with blob-birth zone and with the place where turbulence changes from a drift-wave-type to interchange dominated [3]. On the other hand, analysis of GEMR simulations of AUG plasma indicated that most of the blobs can be actually born more outwards, in the near SOL [3].

Probe diagnostics used on tokamak COMPASS are equipped with a combination of Langmuir (LP) and ball-pen probes (BPP), which allows measurement of plasma potential and electron temperature fluctuations on a microsecond time scale [4], including derived quantities such as electric fields (without parasitic influence of temperature gradients that hinder measurement by LPs only) and particle or heat fluxes. Moreover, the reciprocating probes can penetrate up to several millimeters inside the last closed flux surface and are thus well suited to study characteristics of turbulence both in the scrape-off layer (SOL) and edge of confined plasma.

This work presents an initial study of edge plasma properties at the outer midplane of COMPASS ohmic plasmas using the standard probe-head [5]. In the first part we describe edge plasma profiles and identify two distinct types of fluctuations in the SOL and confined plasma. Second part shows change of properties of the velocity shear layer (VSL) and of some properties of the fluctuations with plasma density.

Fluctuations in the scrape-off layer and confined plasma

Typical edge profiles of the ion saturation current density i_{sat} , electron temperature T_e , radial electric field $E_r = -\partial\phi/\partial r$, poloidal $E \times B$ velocity $v_p = E_r/B_T$ and $E \times B$ shearing rate $|\omega_{E \times B}| = |\partial v_p/\partial r|$ are shown in Fig. 1a) and b). In determination of the plasma potential ϕ we used $\phi = V_{BPP} + 0.6T_e \approx V_{BPP}$ [4], where V_{BPP} is the floating potential of BPP. Due to im-

precision of EFIT magnetic reconstruction the separatrix cannot be determined with sufficient precision and we therefore assume that its position overlaps with position where $E_r = 0$. This allows us to divide the profiles into three regions - *confined plasma* inside $R_{Er=0}$, *near SOL* between $R_{Er=0}$ and the place where the SOL width changes, and the outermost part, *far SOL*.

One-point PDF of density or i_{sat} in SOL can be described by Gamma distribution [1]. PDF of T_e and ϕ is, however, not studied often due to lack of fast measurements. This is possible on COMPASS and shown in Fig. 1d). Clearly, the local fluctuations of the plasma potential follow distribution of i_{sat} , incl. its heavy tail, while PDF of V_{fl} tends to be more symmetric due to influence of temperature fluctuations. Relative fluctuations in the SOL and $\delta T_e/T_e \sim 0.5 - 1 \delta I_{sat}/I_{sat}$

and $\delta\phi/T_e \sim 0.6 - 1$ are somewhat higher than what was reported on other machines: $\delta T_e/T_e \sim 0.4\delta n/n$ and $\delta\phi/T_e \sim 0.3$ [6, 7]. As an indicator of formation of the heavy-tailed PDF, we use difference between mean and mode of the i_{sat} PDF. While they are identical within error bars in the edge, they start to deviate in the near SOL, ~ 2 mm outside of $R_{Er=0}$, due to formation of a significant positive heavy tail of the PDF (marked by the vertical blue dashed line in Fig. 1).

The fluctuations of ϕ and i_{sat} are also correlated in time. This is shown in Fig. 1c) where a phase-shift between the two is plotted in regions with high coherence ($C>0.5$). The phase shift allows us to distinguish two different types of fluctuations. First, the high-frequency branch located in the edge, but protruding also into the near SOL, with phase shift corrected on the poloidal rotation and distance of the probes $\alpha'_{i_{sat},BPP} \approx \pi/4$. Second, low-frequency oscillations forming in the near SOL and extending into the far SOL with $\alpha'_{i_{sat},BPP} \approx \pi/3$ indicating strong interchange component. Both types overlap in the near SOL and bicoherence indicates their

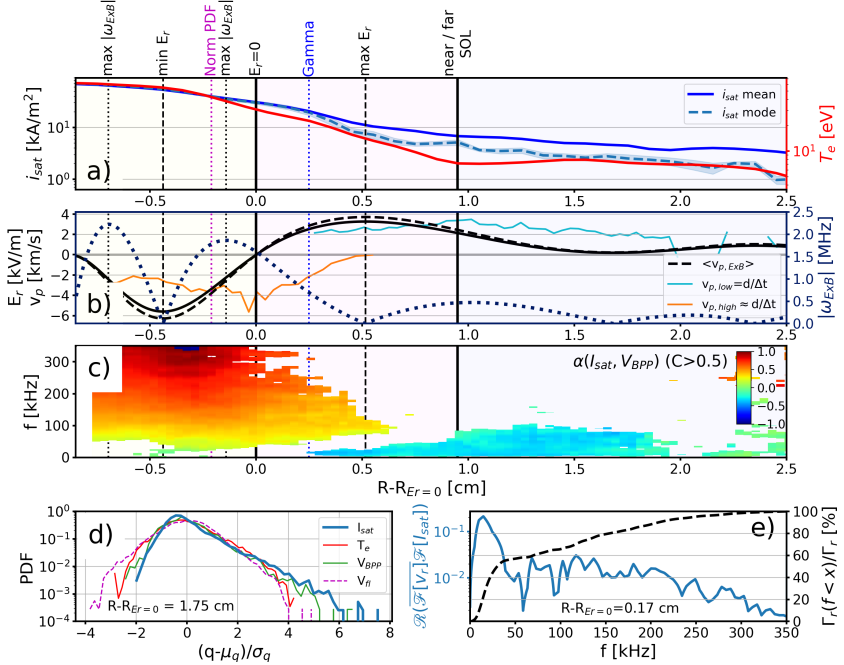


Figure 1: Radial plasma profiles in diverted discharge #6878 ($I_p=180$ kA, $n=4 \cdot 10^{19}$ m $^{-3}$, $B_T=1.15$ T, $q_{95}=4.6$) (a,b) and phase shift between \tilde{I}_{sat} and $\tilde{\phi} \approx \tilde{V}_{BPP}$ (c). v_p of the high-freq. fluctuations (orange) and low-freq. blobs (cyan) is plotted into (b). PDF of measured quantities in the far SOL (d). Spectrally resolved radial particle flux and its cumulative sum in the near SOL (e).

non-linear interaction (not shown here). An estimate of their poloidal velocity computed from a time delay of V_{BPP} measured by two poloidally separated probes at distance $d=8$ mm, band-passed to the frequency range of each respective type, is plotted in Fig. 1b). It shows that in the lab frame both types rotate in the opposite poloidal directions, including the overlap region. The SOL blobs rotate in ion diamagnetic direction.

The inner edge of the low-frequency fluctuations agrees well with the place where the Gamma PDF with clear heavy tail starts to form. Spectral decomposition of the turbulent radial flux $\Gamma_r = \langle \tilde{v}_r \tilde{I}_{sat} \rangle = \int \mathcal{R}(C_{vr,Isat}(f)) df$, where $C(f)$ is the cross-spectral density of the signals [8], is shown in Fig. 1e) for the transition region in the near SOL. While in the edge the radial flux due to the high-frequency fluctuations is dominant, it is gradually damped in the near SOL and the low-frequency peak emerges and takes over most of the radial flux. Central frequency of the peak is 13 kHz and two-point estimate of the poloidal wavelength gives $\lambda_p \sim 15\text{-}20$ cm. This indicates presence of a poloidally rotating structure in the near SOL that modulates one-point measurements at frequency $f = v_p/\lambda_p \approx 2.5$ [km/s] / 0.2 [m] = 12.5 kHz. Time separation of blobs at the near/far SOL boundary (identified as peaks of i_{sat} above level of 2σ) is concentrated around the period of the oscillation, indicating that the structure modulates blob generation.

Density scan

Edge conditions in the previous section were presented for particular plasma parameters. Now we briefly discuss change of properties of the velocity shear layer (VSL), which is considered an important component of turbulence regulation in the edge, with plasma density. In general, typical values observed on the separatrix across COMPASS database are in the range $\phi=20\text{-}80$ V, $T_e=15\text{-}35$ eV, $n=5\text{-}15 \cdot 10^{18} \text{ m}^{-3}$, $|E_{r,max/min}|=2\text{-}8$ kV/m, $|\omega_{E \times B}| < 3 \mu\text{s}^{-1}$. The density scan plotted in Fig. 2 shows that T_e and ϕ at the separatrix decrease linearly with edge density n_{sep} and we observe also linear decrease of the maximal and minimal radial electric fields in the VSL. Since spatial extent of the VSL does not significantly change, the maximal $E \times B$ shearing

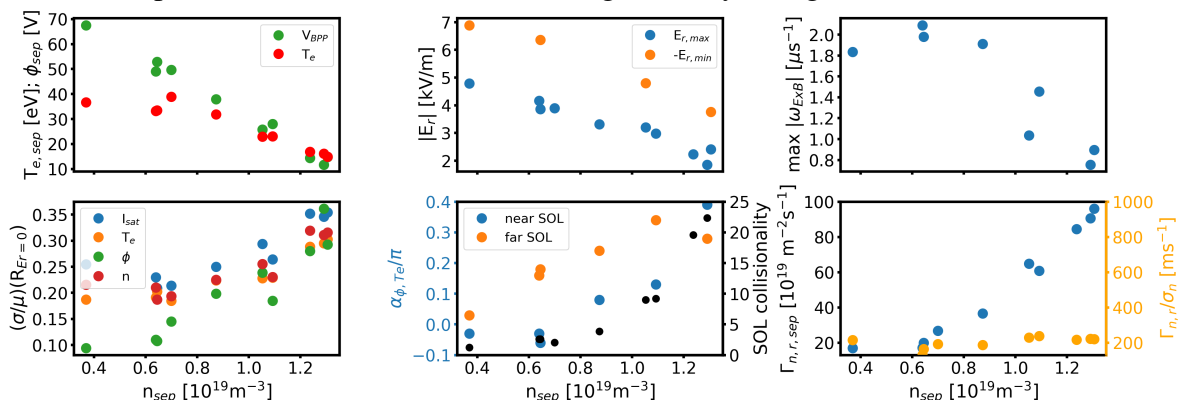


Figure 2: Change of edge plasma properties during density scan. $I_p=180$ kA, $\bar{n}=2.5 \cdot 10^{19} \text{ m}^{-3}$, $B_T=1.15$ T, $q_{95}=3.6$. The line averaged density $\bar{n} \approx n_{sep}/0.13$.

rate around LCFS, and thus capability of the VSL to limit turbulent transport in this region, decreases together with E_r . At the same time the radial particle transport across separatrix increases. This is mainly due to increase of fluctuation amplitude since the flux normalized to the fluctuation amplitude $\Gamma_{n,r}/\sigma_n$ remains constant. Interestingly, we observe also significant increase of phase between fluctuations of ϕ and T_e , α_{ϕ,T_e} , indicating increased cross-field heat transport at higher densities.

Summary

We have identified two distinct types of turbulent fluctuations in COMPASS plasmas, the high-frequency edge oscillations and low-frequency SOL blobs. The transition region is localized in the near SOL, where both types spatially overlap and interact and the radial particle transport gradually transfers from high to low frequencies. Even though skewness of i_{sat} fluctuations is positive even inside LCFS, distinguishable Gamma-distributed PDF, formed by the low-frequency fluctuations, arises in the near SOL. This supports, together with turbulence spreading rate being positive in the near SOL but negative in the edge, the picture presented in [3] that most of the fluctuations that form a positive skewness in the edge region disappear around LCFS and new blobs are formed in the near SOL.

Further, we cannot confirm the assumption that the blobs are generated randomly according to a Poisson process. Oscillations of all measured quantities, incl. radial particle flux, in the near SOL are peaked around ~ 13 kHz. This seems to correspond to a poloidally rotating structure with a rather large poloidal wave-length $\sim 15 - 20$ cm, that at least partly modulates blob generation. Nevertheless, we note that time separation of blobs becomes more random further in the SOL, possibly due to differences in their individual propagation.

These observations hold for diverted plasmas, but the situation may be different in limited low-elongation plasmas where the radius of zero skewness was observed to be shifted significantly (several cm) inwards, compared to diverted configuration, and Gamma-like PDF is detected even inside the LCFS. Study of these plasmas is ongoing.

Acknowledgement. This work was supported by the project of the Czech Science Foundation GA16-25074S and co-funded by MEYS projects number 8D15001 and LM2015045.

References

- [1] D.A. D'Ippolito, et al., *Phys. Plasmas* **18**, 060501 (2011)
- [2] O.E. Garcia, *Phys. Rev. Lett.* **108**, 265001 (2012)
- [3] P. Manz, et al., *Phys. Plasmas* **22**, 022308 (2015)
- [4] J. Adamek, et al., *Rev. Sci. Instr.* **87**, 043510 (2016)
- [5] J. Adamek, et al., *Contrib. Plasma Phys.* **54**, 279 (2014)
- [6] J.A. Boedo, et al., *Jour. Nucl. Mater.* **390-391**, 29 (2009)
- [7] J. Horacek, et al., *Nucl. Fusion* **50**, 105001 (2010)
- [8] O. Grover, et al., *Rev. Sci. Instr.* **88**, 063501 (2017)